

DeltaFlex: an Additively Manufactured Monolithic Delta Robot with Compliant Joints

Alberto Parmiggiani¹, Emilio Ottonello^{1,2}, Seyyed Masoud Kargar³,
Mario Baggetta³, Guangbo Hao⁴, and Giovanni Berselli^{1,3},

¹ Fondazione Istituto Italiano di Tecnologia (IIT),
Via S. Quirico 19/D, 16163 Genova, Italy

² Dipartimento di Informatica, Bioingegneria, Robotica e
Ingegneria dei Sistemi [DIBRIS],

Università degli Studi di Genova, Via Opera Pia 13, Genova, 16145, Italy

³ Dipartimento di Ingegneria Meccanica [DIME],

Università degli Studi di Genova, Via Opera Pia 15, Genova, 16145, Italy

⁴ School of Engineering and Architecture-Electrical and Electronic Engineering,
University College Cork, College Road, Cork, Ireland

Abstract

This study presents the design and validation of a compliant Delta robot created through additive manufacturing (AM) with a monolithic structure. The use of AM expedites the development cycle of robots, enabling faster prototype development and deployment, as well as facilitating experimentation with new robot kinematics. The use of compliant joints poses a challenge in achieving substantial workspaces for robots. However, parallel architectures are well-suited for implementing flexible joints because they require lower ranges of motion for individual joints than serial architectures. Thus the Delta configuration was chosen for this study. A Design for Additive Manufacturing (DfAM) strategy was adopted to minimize the need for support structures and maximize mechanical strength. The overall performance of the Delta was evaluated quantitatively in terms of stiffness and precision. The stiffness test aimed to measure the device's capability to withstand applied loads, while the repeatability test assessed the robot's precision and accuracy. Moreover, FEM verification was adopted. Structural simulations are a powerful tool for verifying the experimental results of a robotic system. The approach presented in this work offers an interesting avenue for robot design with significant

potential for future advancements and practical applications and sheds light on the trade-offs that designers should consider when adopting this methodology.

Introduction

One of the most studied and widely used parallel manipulators is the Delta robot introduced by Clavel [1] in the early 80's. This parallel robot has three actuators mounted on the base, which move three parallel arms connected to a platform which is used as end-effector. Each arm has an active link connected to the base through a revolute joint and a passive one connected to the platform through four universal or spherical joints. These kinematic chains restrict the motion of the platform but in its three translational degrees of freedom. The Delta robot is known for its light structure, high speed, and high accuracy, which make it suitable for applications such as packaging and pick-and-place operations [2].

The Delta robot architecture has proven to be highly versatile and adaptable, as demonstrated by its continued use in various novel applications across a wide range of fields. A few recent examples can be found in the work of Tran et al. [3] who equipped a Delta robot with an image processor to classify products and rapidly pick and drop them in a classification box or in the work of Xiao et al. [4] that used a Delta robot in a robot-assisted retinal surgery system. Okunevic et al. [5] developed the DeltaCharger, a system based on Delta kinematics that can precisely position a set of electrodes to transfer energy between two robots. Hirano et al. [6] built a Delta robot driven by pneumatic artificial muscles. According to the authors, this device could be a rehabilitation and VR/AR haptic device.

The work by McClintock et al. [7] is interesting as it presents one of the first comprehensive implementations of compliant joints for parallel robots, namely the milliDelta, which was fabricated via the PC-MEMS [8] technique at the millimeter-scale. The authors demonstrated that the milliDelta system can achieve precise motion of the payload relative to the workspace.

While the work of McClintock et al. is noteworthy, their focus was primarily on the "micro" scale, and only a few "meso" scale implementations have been reported to date. As such, the fabrication of compliant robots remains an open question. In this study, we explore the use of additive manufacturing (AM) technology to build a delta robot at the "meso" scale, motivated by a curiosity-driven approach.

Compliant mechanisms, which replace joints with compliant elements

such as flexure hinges or elastic bearings, have been extensively studied over the past two decades. Howell's [9], [10] and Lobontiu's [11] books offer comprehensive overviews of compliant mechanisms, including design approaches, guidelines, and examples of their applications. In any case, despite the practical relevance, investigations on spatial, rather than planar, compliant mechanisms are quite limited. As instances, Smith [12] proposed compliant universal joints fabricated from circular leaf springs, Callegari et al. [13] addressed the analysis and design of a spherical parallel mechanism with flexure hinges, Parvari Rad et al. [14], proposed and optimize a spherical flexural hinge to achieve spatial motions.

In this scenario, AM enables great design freedom and cost-effectiveness, making it a valuable tool for creating compliant joints that are difficult or impossible to manufacture with traditional methods. However, the application of compliant mechanisms poses unique challenges. Most mechanical systems require significant ranges of motion, which can be difficult to achieve with compliant mechanisms due to their strain affecting their durability and robustness. Therefore, it is important to consider the available solutions in the literature to address this problem.

For instance, Fowler et al. presented an evolution of the "butterfly-hinge" design by Henein et al.[15], which was fabricated using AM in titanium [16]. Merriam et al. developed a monolithic 2DOF pointing mechanism [17] for space applications, while Kiener et al. presented the construction of a flex-type pivot with interlocked flexure blades [18] and a compliant rotation reduction mechanism.

In addition to utilizing metal components, AM can also facilitate the fabrication of compliant joints with plastic materials, that have the advantageous capability of accommodating larger strains, thereby enabling larger displacements than metals. For example, Sharkey et al. [19] presented a monolithic 3D-printed flexure translation stage, fabricated using Fused Filament Fabrication (FFF), that forms the key element of an open-source miniature microscope. Similarly, Almeida et al. [20] presented a 3D-printed flexure-based robotic micropipettes device for precision manipulation that was obtained using Selective Laser Sintering (SLS). These examples demonstrate the versatility of AM in the design and fabrication of compliant joints, and its potential to create large displacement joints for various applications, including aerospace, medical and robotic.

The freedom in the design phase provided by additive manufacturing allows for the creation of *non-assembly mechanisms* [21], which do not require any assembly operations. These mechanisms are unique as they can be used immediately after being manufactured. Adopting these mechanisms

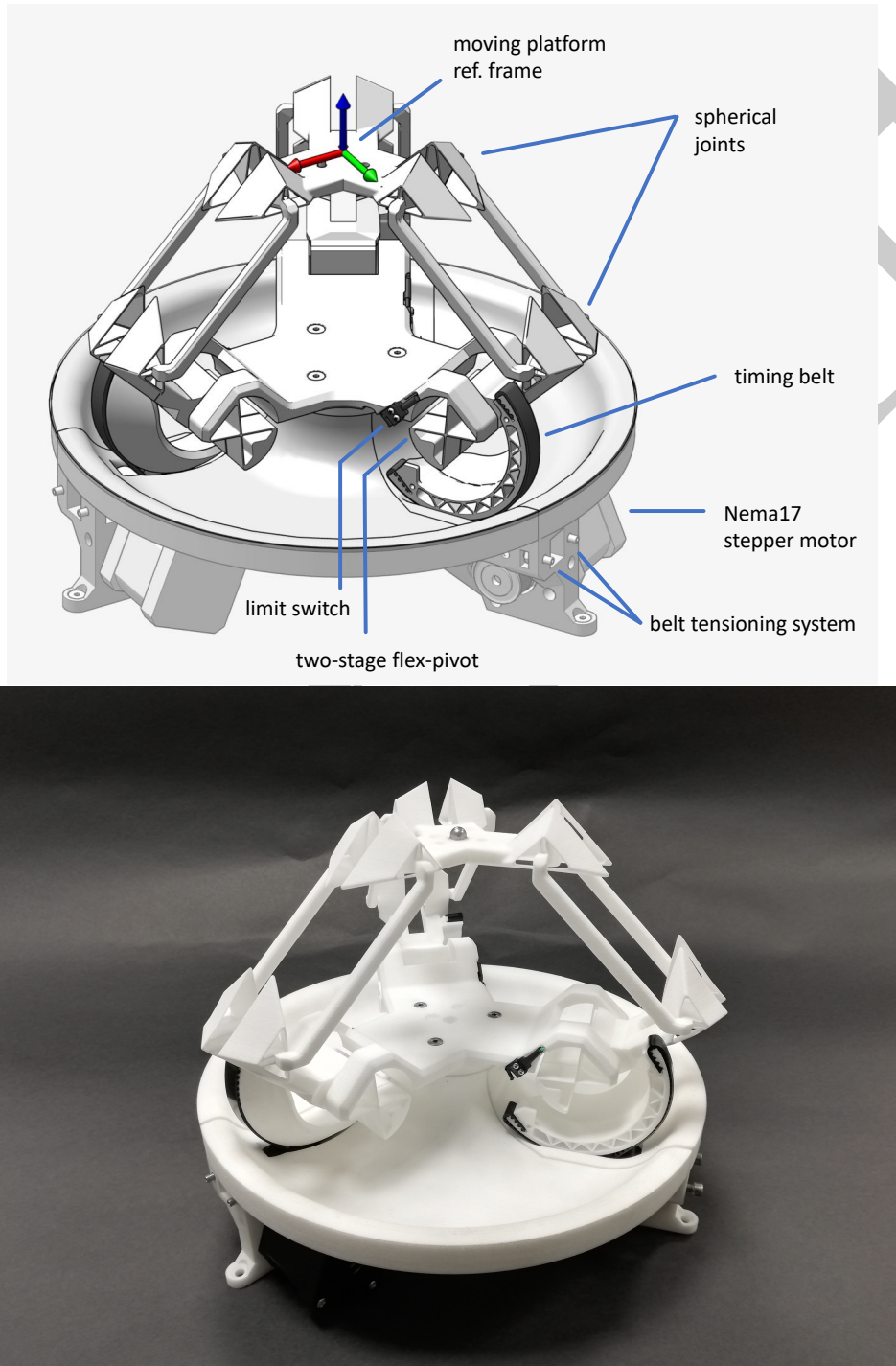


Figure 1: CAD view and photograph of the DeltaFlex

has several benefits such as time and cost savings due to the elimination of assembly operations, no tight tolerances to be respected, and no need for screws, bearings or fasteners, resulting in weight reduction. These advantages make non-assembly mechanisms a viable option for certain applications where time and cost efficiency are crucial.

Above all, this study draws inspiration from three works: Bruyas et al. [22], Rommers et al. [23], and Naves et al. [24]. The work of Bruyas et al. [22] is significant for being one of the earliest to present a 2DOF mechanism fabricated monolithically using multi-material printers. In 2021, Rommers et al. [23] introduced the “Tetra 1” and “Tetra 2” designs for large range of motion spherical joints, with the latter being particularly well-suited for additive manufacturing and used as one of the key building blocks of the current work. Additionally, Naves et al. [24] recently demonstrated the feasibility of high-precision parallel robots with large workspaces, utilizing only compliant joints. Some of the key concepts from these works were adapted and integrated into the present work.

The goal of this study is to design and validate a Delta robot created through AM with two fundamental characteristics: its structure is monolithic and its joints are compliant. The significance of this study lies in the fact that AM expedites the development cycles of robots, which can be advantageous for various purposes. For instance, this approach could facilitate the acceleration of prototype development and deployment, enable experimentation with new robot kinematics, and permit robot construction even in scenarios where off-the-shelf components are unavailable (e.g. in the case of supply chain disruptions). The practical implementation of this approach, as presented in this work, sheds light on the trade-offs that designers must confront should they choose to adopt this methodology.

System design and implementation

Compliant joints typically exhibit restricted ranges of motion, posing a considerable challenge in achieving substantial workspaces for robots. Parallel architectures are, however, particularly well-suited for implementations with flexible joints (as the work of Naves et al. [24] demonstrates), given that the required range of motion for individual joints is often lesser than that required for serial architectures. In light of the aforementioned considerations, the Delta architecture was selected for this study. The system implementation is represented in Fig.1 which shows an overall view of the DeltaFlex and its main parts.

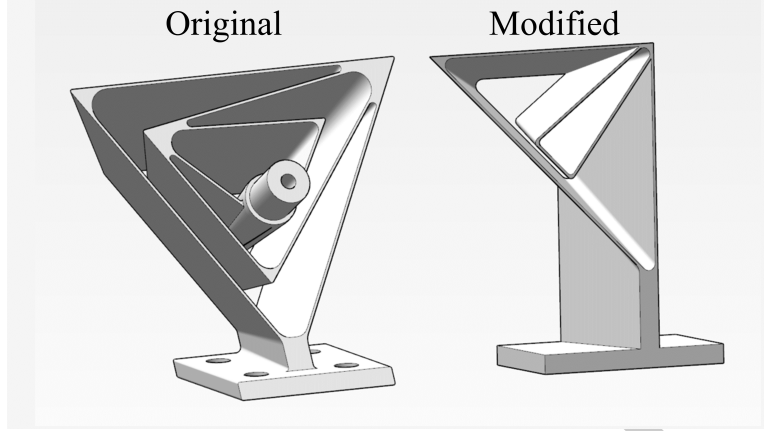


Figure 2: Comparison between adopted spherical joint and the one designed by Rommers et al. [23]

Notwithstanding the parallel architecture, achieving extensive ranges of motion for the joints remained challenging. To address this issue, a two-stage cross flex-pivot was utilized for implementing the rotational (R) joint of each arm in the base. For the same reason, the four spherical joints of each arm were constructed with a design drawing inspiration from the “Tetra2” joint developed by Rommers et al. [23], albeit with some slight modifications to enhance the range of motion and prevent self-collisions. Fig.2 represents the joint developed by Rommers et al. and the spherical joint adopted for the DeltaFlex.

Moreover, a Design for Additive Manufacturing (DfAM) strategy was adopted for the entire robot. Specifically, all the flexures in each arm were designed to develop orthogonally to a shared orientation. Selecting this direction as the build direction maximizes the mechanical strength of each flexure. To reduce the need for support structures, horizontal geometric features were gradually extended from the side surfaces at an inclination exceeding 45° , rendering them self-supporting. Additionally, features exhibiting overhangs were eliminated wherever feasible. In this study, selective laser sintering (SLS) was chosen as the manufacturing technology due to its cost-effectiveness and because it does not require the addition of support structures. However, owing to the DfAM methodology employed, the geometry obtained is also well-suited for fused filament fabrication (FFF) printers, which are more prevalent. The robot was manufactured on a 3D Systems ProX SLS 6100 machine with Duraform as construction material.

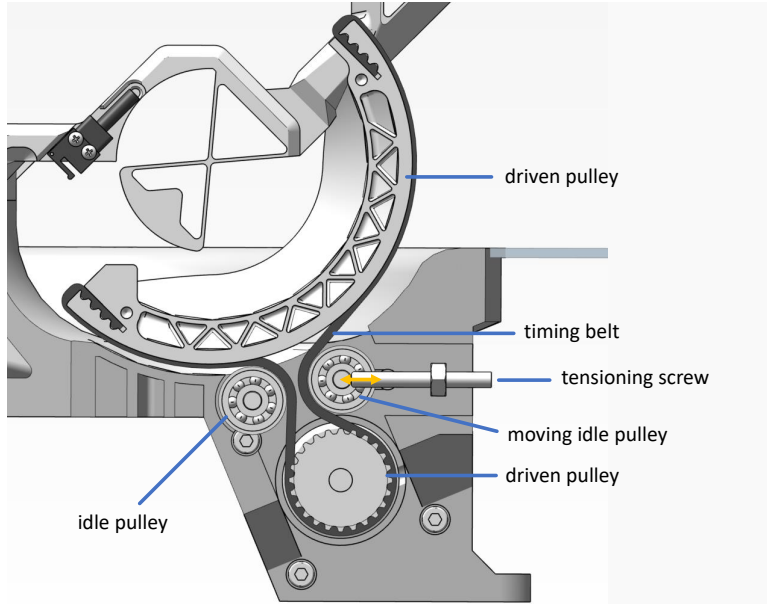


Figure 3: Belt tensioning mechanism

Duraform PA is a durable polyammide 12 thermoplastic (a.k.a. Nylon) with good structural properties which also exhibits close to isotropic behaviour once manufactured. Furthermore the high value of deformation at break (14%) makes this material particularly suitable for the construction of compliant mechanisms. All flexures were designed with a thickness of 0.7[mm], which was found to be the lowest thickness value that could be reliably manufactured on the ProX SLS 6100.

The actuation of each arm was achieved through the use Nema17 stepper motors, because of their high holding torque and ease of control. The motors used for this device had a step angle of 1.8° , a holding torque of 0.59[Nm] and an input voltage of 2.80[V]. The driving motors were connected to a driven pulley integrated directly on the first link of each arm with a timing belt, thus achieving a transmission ratio of 3.8:1. The belt tensioning system (represented with its components in detail in Fig.3) was integrated directly in the support structure of the device.

The motors were controlled with an Arduino UNO WIFI rev.2 (ATmega4809 8-bit microcontroller) and a 3-Axis CNC/Stepper Motor Shield that controlled the motors through A4988 stepper drivers. An Omron D2MQ-4L-105-1 limit-switch was installed on each axis to achieve the initial homing of the device. To facilitate the replication of this study, all models

and materials have been made accessible on a GitHub repository ¹.

Experiments

The overall performance of the DeltaFlex was quantitatively evaluated focusing on two main aspects: stiffness and precision. The assessment of stiffness aimed at measuring the capability of the device to withstand applied loads which is, in turn, important to maintain motion precision in different operating conditions. While this is not usually a major problem for conventionally designed robots with rigid links and bearings it becomes particularly relevant in the case of robots with compliant joints. The stiffness of the device was characterized with a *Zwick-Roell Z050* tensile/compression testing machine, equipped with a load cell rated for 50[kN] full-scale load (with Class 1 accuracy in the ISO 7500-1 standard). During the tests, the base of the robot was kept fixed, while the end-effector was locked to the moving traverse. The traverse speed was set to the constant value of 0.5[mm/s]. During this process the traverse caused the robot to deform while the resulting forces and displacements were recorded. Two different configurations were tested: in the first, the robot was installed with the moving platform perpendicular to the direction of movement of the moving traverse, while in the second configuration, the moving platform was kept parallel to the direction of movement of the moving traverse. Fig. 4 represents these configurations. Starting from the home configuration, both loading conditions were applied bidirectionally by performing both descending and ascending movements of the moving traverse. This allowed evaluating the behavior of the robot in opposite directions. To obtain statistical data, the test was replicated five times in all conditions and the outcomes were averaged.

Finally, the second test was performed to assess the repeatability of the robot. This performance indicator is critical for applications that require high precision and accuracy (e.g. the manufacturing industry). To do so, the robot's end-effector was moved to six different reference configurations close to the limits of the robot's workspace for twenty repetitions. In each repetition, the final position of the end-effector was measured with a *TESA 01811001 SwissTast* micrometric dial gauge (range: 0.2[mm], resolution: 0.002[mm], measuring force: 0.15[N]). To attain reproducibility of the test, the probe made contact with an 8[mm] diameter calibrated, hardened stainless-steel sphere. The experimental setup is shown in Fig.5.

¹<https://made-iit.github.io/deltaflex/>

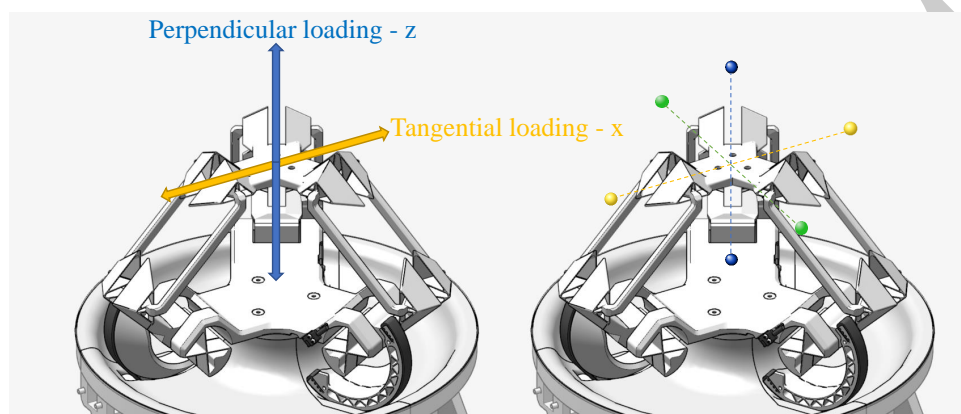


Figure 4: Different load configurations and reference configurations

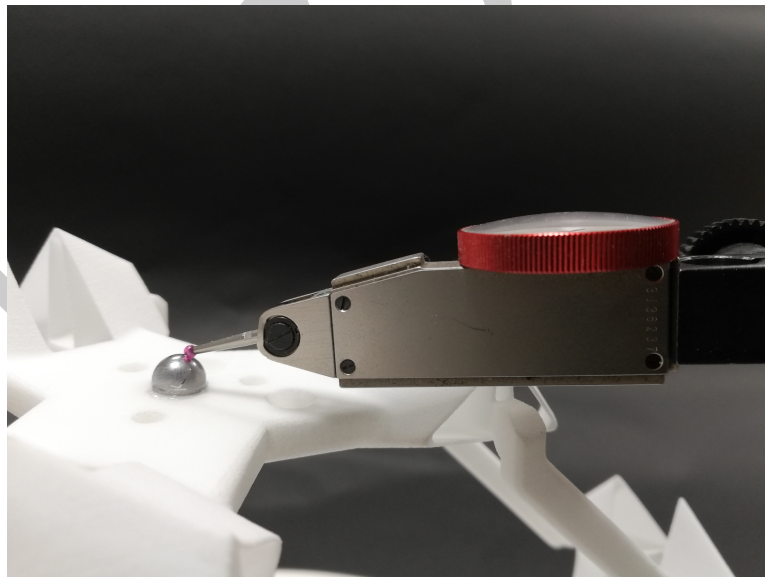


Figure 5: Repeatability test setup

Results

The results of the stiffness test are represented in Fig.6.a) for the case of loading directed perpendicularly to the end-effector, and in Fig.6.(b) for the case of transversal loading. In both cases the ascending load path (robot subject to traction force) and the descending load path (robot subject to compression force) are represented in green and blue respectively. The curves represent the average of all the experimental runs while the shaded bands above and below the curve represent the standard deviation of the experimental data. Arrows were superimposed to the plots to indicate the sections of the curves that correspond to the increasing load and decreasing load phases. A linear fit of the force-displacement curve in the perpendicular loading case yields a stiffness value of 0.41[N/mm]; for the tangential loading case the computed stiffness is 0.19[N/mm].

A first observation is that in each condition the loading and unloading of the robot do not follow the exact same force-displacement trajectory; this gives rise to a narrow hysteresis loop. This is somewhat surprising considering there are no bearings with relatively moving parts and all robot motion is due to the flexures' deflection which should be nearly frictionless. We therefore attribute this effect to the internal material friction of additively manufactured flexible components.

Secondly, the force-displacement curve is not perfectly linear. This effect could be due to either the effect of large deformation or to non-linear material properties. Further testing will be required to ascertain what phenomenon causes this effect.

Despite these drawbacks, the overall value of stiffness of the robot is relatively low and the DeltaFlex achieves a significant range of motion while opposing a rather low resistance to motion.

The results of the repeatability test are shown in Fig.7. The plot shows how for the four chosen configuration the average position shift is less than 30[μ mm], indicating good repeatability.

FEM simulation

Structural simulations are a powerful tool for verifying the experimental results of a robotic system. In this case, the aim is to simulate the DeltaFlex robot using RecurDyn, a multibody dynamics software, and evaluate its stiffness properties. By modeling the robot in a virtual environment, its behavior can be studied, and the simulation results can be compared with

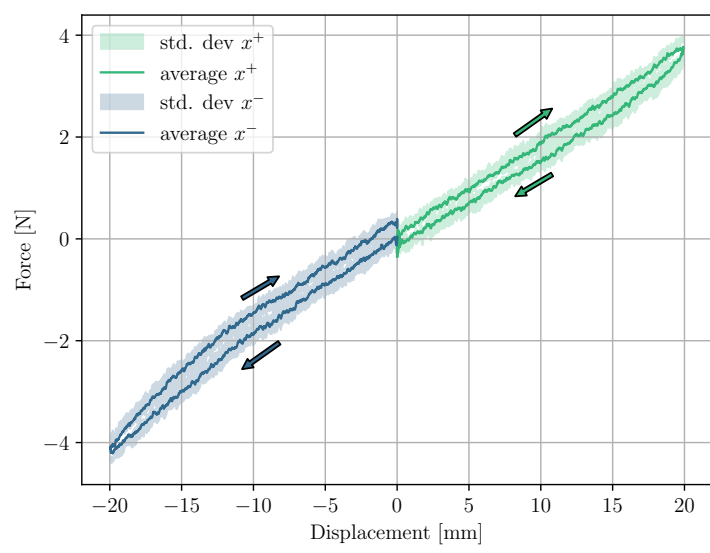
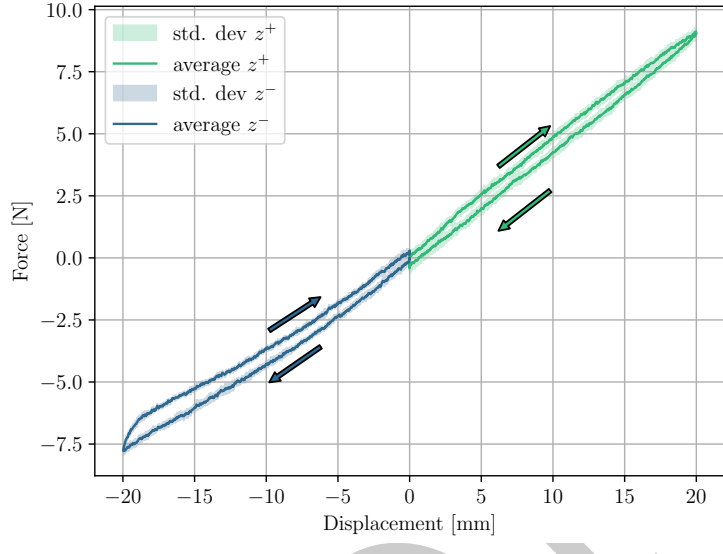


Figure 6: Experimental results of the stiffness tests. a) Represents the force-displacement curve for the case of perpendicular loading. b) Represents the force-displacement curve for the case of tangential loading.

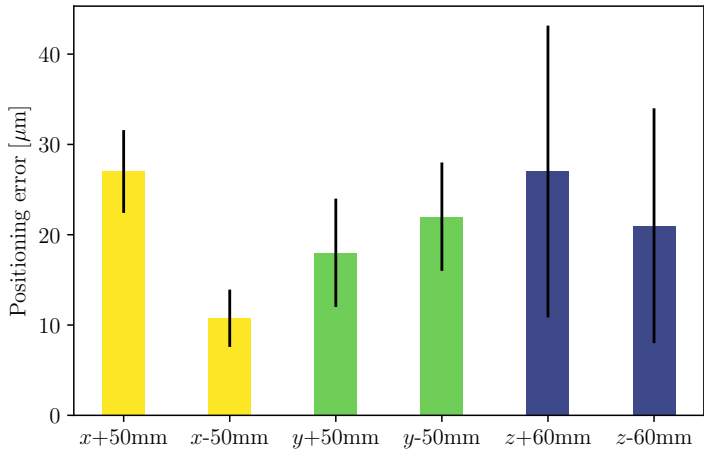


Figure 7: Histograms of the repeatability errors and standard deviations for the six reference configurations.

the experimental data to make informed decisions in the design process.

To perform the simulation, the 3D model designed in PTC Creo was imported into RecurDyn, as can be seen in Fig.8 and assigned the material properties for Nylon from RecurDyn’s library. The links, base, and end-effector were treated as rigid bodies. The flexures were meshed using a minimum and maximum mesh size of 0.2 and 1.2, respectively, and a triangular mesh (shell element) was chosen for the mesh type. To replicate the experiments ± 20 mm displacement in both horizontal and vertical directions were defined with a point on curve (PTCV) joint. The reaction forces on the joint were measured for the input displacement to plot the force-displacement graphs for both cases, as shown in Fig.9.

It should be noted that, in the simulations, the value of Young’s modulus that matched the experimental results was of 1000[MPa]. This value is 27% lower than the value of 1387[MPa] stated in the manufacturer’s datasheet. The difference in mechanical properties could potentially be linked to modifications in the microstructural morphology of the material during high-temperature printing, non-linear elastic behaviour. A comprehensive and thorough evaluation of the material through material testing would be essential to corroborate this hypothesis (but is beyond the scope of the current work).

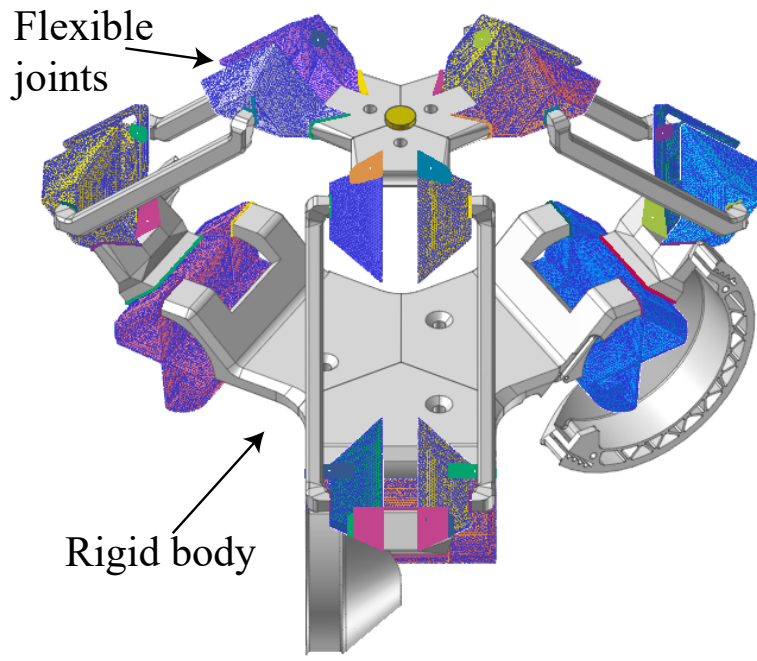
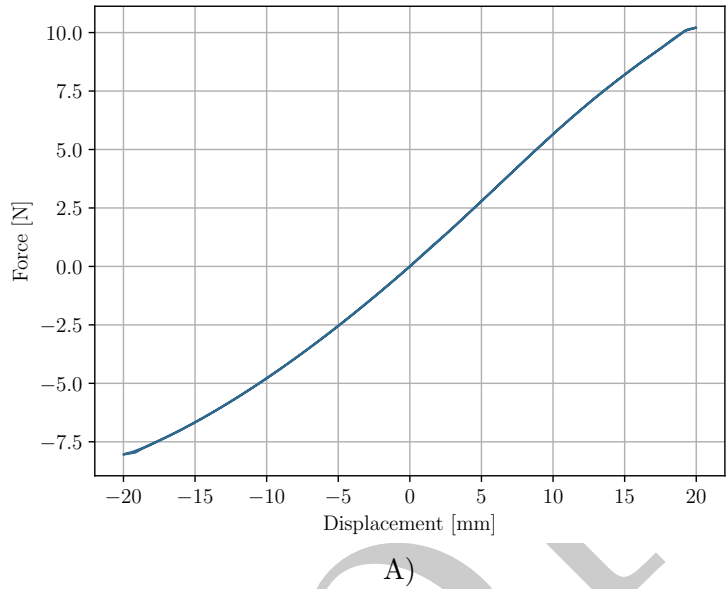
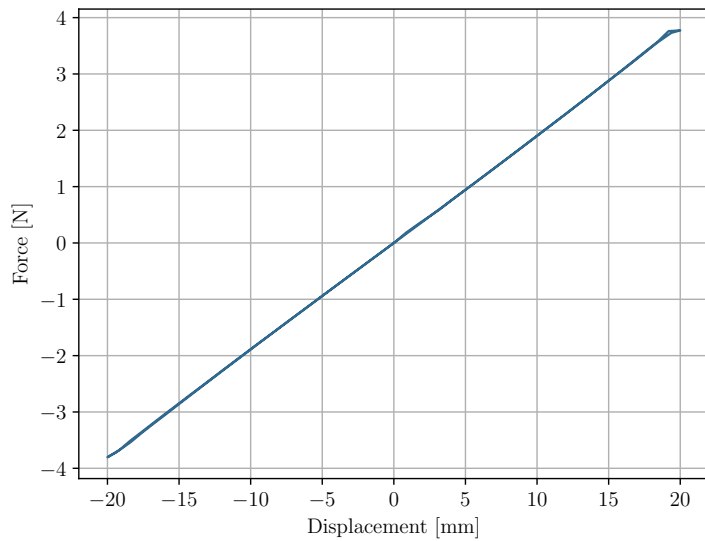


Figure 8: 3D hybrid model developed within the Recurdyn environment that was used for the simulations. The meshed regions correspond to the flexible parts of the model, whilst the grey parts represent the indeformable solid bodies.



A)



B)

Figure 9: Results of the stiffness simulations in RecurDyn. a) Represents the force-displacement curve for the case of perpendicular loading. b) Represents the force-displacement curve for the case of tangential loading.

The force-displacement curve for the horizontal loading case was linear and did not show the slight non-linearity of the experimental results. The force-displacement curve for the vertical loading case showed a slight non-linearity that could be attributed to the effect of large deformations.

Conclusions and Future developments

The tests that were performed provide an assessment of the robot's main characteristics, highlighting its low stiffness, resulting in low resistance to motion and high repeatability. These observations indicate that the DeltaFlex holds promise for utilization in a diverse range of applications where precision and accuracy are required. Furthermore, the experimental results revealed potential areas for optimization and improvement.

In the current prototype, stepper motors were utilized for actuation. However, in future iterations, the actuation system may be improved by incorporating brushless DC (BLDC) motors and low gear ratios. This change would enable the implementation of torque control during interaction tasks, thus enhancing the precision and versatility of the system.

Further work shall involve thorough examination of the fatigue life of flexures, as a function of the applied loads and the number of loading cycles. Additionally, efforts may be directed towards exploring alternative materials and fabrication technologies, such as Fused Filament Fabrication (FFF), to further augment the current understanding.

In summary, despite the aforementioned minor inconveniences, we assert that the approach presented in this work offers an interesting avenue for robot design with significant prospects for future advancements, as well as a captivating potential for practical applications.

Acknowledgments

We thank the staff of the IIT MWS facility (especially Lorenzo Orciari, Roberto Puddu, Marco Pinaffo and Angela Morelli) for their support in the construction of the prototypes. We thank the anonymous reviewers whose suggestions helped significantly improve the manuscript.

References

- [1] Clavel, R., 1987. Device for displacing and positioning an element in space, WIPO Patent WO1987003528A1.

- [2] Staicu, S., 2019. *Dynamics of Parallel Robots*. Springer International Publishing.
- [3] Do, T. V., City, H. C. M., Viet, N. Q., Nam, N. Q., Dat, P. N., Vinh, D. D., and Hung, T. V., 2021. “Design of delta robot using image processing for product sorting process”. *2021 International Conference on System Science and Engineering (ICSSE)*, 8, pp. 210–214.
- [4] Xiao, B., Alamdar, A., Song, K., Ebrahimi, A., Gehlbach, P., Taylor, R. H., and Iordachita, I., 2022. “Delta robot kinematic calibration for precise robot-assisted retinal surgery”. *2022 International Symposium on Medical Robotics, ISMR 2022*.
- [5] Okunovich, I., Trinitatova, D., Kopanov, P., and Tsetserukou, D., 2021. “Deltacharger: Charging robot with inverted delta mechanism and cnn-driven high fidelity tactile perception for precise 3d positioning”. *IEEE Robotics and Automation Letters*, **6**, 10, pp. 7604–7610.
- [6] Hirano, J., Tanaka, D., Watanabe, T., and Nakamura, T., 2014. “Development of delta robot driven by pneumatic artificial muscles”. *2014 IEEE/ASME International Conference on Advanced Intelligent Mechatronics*, 7, pp. 1400–1405.
- [7] Mcclintock, H., Fatma, Temel, Z., Doshi, N., Koh, J.-S., and Wood, R. J., 2018. “The millidelta: A high-bandwidth, high-precision, millimeter-scale delta robot”. *Science Robotics*, **3**, 1.
- [8] Sreetharan, P. S., Whitney, J. P., Strauss, M. D., and Wood, R. J., 2012. “Monolithic fabrication of millimeter-scale machines”. *Journal of Micromechanics and Microengineering*, **22**, 4, p. 055027.
- [9] Howell, L. L., 2001. *Compliant Mechanisms*. John Wiley and Sons.
- [10] Howell, L. L., Magleby, S. P., and Olsen, B. M., 2013. *Handbook of Compliant Mechanisms*. John Wiley and Sons.
- [11] Lobontiu, N., 2001. *Compliant Mechanisms : Design of Flexure Hinges*. CRC Press, 11.
- [12] Smith, S. T., 2000. *Flexures: Elements of Elastic Mechanisms*. CRC Press.
- [13] Callegari, M., Cammarata, A., Gabrielli, A., Ruggiu, M., and Sinatra, R., 2009. “Analysis and Design of a Spherical Micromechanism With Flexure Hinges”. *Journal of Mechanical Design*, **131**(5).

- [14] Parvari Rad, F., Vertechy, R., Berselli, G., and Parenti-Castelli, V., 2016. “Analytical compliance analysis and finite element verification of spherical flexure hinges for spatial compliant mechanisms”. *Mechanism and Machine Theory*, **101**, pp. 168–180.
- [15] Henein, S., Spanoudakis, P., Droz, S., Myklebust, L. I., and Onillon, E., 2003. “Flexure pivot for aerospace mechanisms”. In 10th European Space Mechanisms and Tribology Symposium, pp. 285–288.
- [16] Fowler, R. M., Maselli, A., Pluimers, P., Magleby, S. P., and Howell, L. L., 2014. “Flex-16: A large-displacement monolithic compliant rotational hinge”. *Mechanism and Machine Theory*, **82**, 12, pp. 203–217.
- [17] Merriam, E. G., Jones, J. E., Magleby, S. P., and Howell, L. L., 2013. “Monolithic 2 dof fully compliant space pointing mechanism”. *Mechanical Sciences*, **4**, pp. 381–390.
- [18] Kiener, L., Saudan, H., Cosandier, F., Perruchoud, G., and Spanoudakis, P., 2019. “Innovative concept of compliant mechanisms made by additive manufacturing”. *MATEC Web of Conferences*, **304**, 1, p. 7002.
- [19] Sharkey, J. P., Foo, D. C., Kabla, A., Baumberg, J. J., and Bowman, R. W., 2016. “A one-piece 3d printed flexure translation stage for open-source microscopy”. *Review of Scientific Instruments*, **87**, 2, p. 025104.
- [20] Almeida, A., Andrews, G., Jaiswal, D., and Hoshino, K., 2019. “The actuation mechanism of 3d printed flexure-based robotic microtweezers”. *Micromachines*, **10**, 1, p. 470.
- [21] Lussenburg, K., Sakes, A., and Breedveld, P., 2021. “Design of non-assembly mechanisms: A state-of-the-art review”. *Additive Manufacturing*, **39**, p. 101846.
- [22] Bruyas, A., Geiskopf, F., Meylheuc, L., and Renaud, P., 2014. “Combining multi-material rapid prototyping and pseudo-rigid body modeling for a new compliant mechanism”. In Proc. IEEE Int. Conf. on Robotics and Automation (ICRA), pp. 3390–3396.
- [23] Rommers, J., van der Wijk, V., and Herder, J. L., 2021. “A new type of spherical flexure joint based on tetrahedron elements”. *Precision Engineering*, **71**, pp. 130–140.

- [24] Naves, M., Nijenhuis, M., Seinhorst, B., Hakvoort, W., and Brouwer, D., 2021. “T-flex: A fully flexure-based large range of motion precision hexapod”. *Precision Engineering*, **72**, pp. 912–928.

Preprint